2013

Synthesis and Characterization of pH-Responsive Elastin-Like Polypeptides with Different Configurations

Mingjie Tang
Cleveland State University

SYNTHESIS AND CHARACTERIZATION OF pH-RESPONSIVE ELASTIN-LIKE POLYPEPTIDES WITH DIFFERENT CONFIGURATIONS

MINGJIE TANG

Bachelor of Science in Chemical Engineering

North University of China

June 2010

submitted in partial fulfillment for the degree

Master of Science in Chemical Engineering

at the

Cleveland State University

August 2013

This thesis has been approved for the department of Chemical & Biomedical Engineering and the College of Graduate studies by

---

Nolan B. Holland, Ph. D.

Department of Chemical & Biomedical Engineering

_____

Date

Chandra Kothapalli, Ph. D.

Department of Chemical & Biomedical Engineering

_____

Date

Surendra N. Tewari, Ph. D.

Department of Chemical & Biomedical Engineering

_____

Date

Aimin Zhou, Ph. D.

Department of Chemistry

_____

Date

ACKNOWLEDGEMENT

Foremost, I would like to express my sincere gratitude to my advisor Dr. Nolan Holland, for the continuous support of my master study and research, for his patience, motivation, enthusiasm, and immense knowledge. His guidance helped me in all the time of research and writing of this thesis. It has been a wonderful experience for me working in his laboratory and under this guidance.

I would like to thank Dr. Zhou and Dr. Tewari for taking the time to be on my committee. Also thank Dr. Chandra for offering inspiring and interesting information on his biomaterials and biomechanics courses.

My lab mates in Dr. Holland`s laboratory have been of great assistance to me over these years. Special thanks to Jim Cole, he trained me when I first joined this Lab, and helped me to better understand my research and provide valuable insights. I will be forever grateful for his help and wish him the best in his further career.

Special thanks to Ms. Becky Laird and Darlene Montgomery for their support throughout my time at Cleveland State University. Ms. Laird has helped me through many tough times by motivating me and providing valuable insights.

Thank my parents, without their support; I would not be able to finish my education. Special thanks to my fiancée, Jingjing Wang. She is always supporting throughout my study.

SYNTHESIS AND CHARACTERIZATION OF pH-RESPONSIVE ELASTIN-LIKE POLYPEPTIDES WITH DIFFERENT CONFIGURATIONS

MINGJIE TANG

ABSTRACT

Elastin-like polypeptides (ELP) are environmentally responsive polymers that exhibit phase transition behavior in response to various stimuli such as temperature, pH and irradiation. In this work, we focused on pH-responsive ELPs. It has been shown that pH value, configurations of ELPs, ELP concentration, and salt concentration can impact the phase transition behavior of pH-responsive ELPs. Quantitative models have been developed to engineer various linear ELPs, but there has not been any detailed study for engineering ionizable ELP with non-linear configurations.

In this study, we designed, synthesized, and characterized pH-responsive ELPs with two different configurations. One is linear ELP, $(GVGVPGEGVPGVGVP)_{12}$, and the other one is a three-armed star ELP, $(GVGVPGEGVPGVGVP)_{12}$-foldon. Three ELP-foldon chains fold as a trimer in solutions. These constructs were synthesized by molecular biology techniques and characterized by different methods.

A modified model based on previous studies was used to describe the pH-dependent reversible phase transition in response to their solution environment. The model was validated with pH-responsive ELPs with different configurations, i.e., linear and trimer. The phase transition of both ELPs fit this model across a range of pH. These results demonstrate that we are able to rationally design responsive polypeptides with different configurations whose transition can be triggered at a specified pH.

TABLE OF CONTENTS

LIST OF FIGURES

CHAPTER I

INTRODUCTION

1.1 Overview

In recent years, macromolecules have emerged as excellent candidates to create highly functional materials [1]. With the availability of thousands of different monomers, and the possibilities opened by their different combinations, polymer scientists have developed a tremendous amount of materials for various applications.

The concept of responsive materials has begun to attract attention and has boosted expectations for new applications. This concept is inspired by living systems, which respond to external stimuli by adapting to changing conditions. The "smart" polymers, or responsive polymers, are materials that may have dramatic property changes in response to small changes in the environment. This new class of polymer often requires a high level of control of its compositions. However, all traditional methodologies of polymer synthesis are characterized by an unavoidable component of randomness and lack of control. For radical, cationic, or ring-opening polymerization, even in the simplest polymers, it is not possible to control parameters such as degree of polymerization. Furthermore, polymers and the synthesis methodologies are almost always based on

petroleum-derived chemicals. This resource is neither renewable nor environmental friendly [2].

Peptide-based "smart" polymers normally are soft and wet, due to their high hydration, which makes them an ideal candidate for applications that necessitate bringing these materials into contact with an aqueous environment, the degree of hydration can be profitably exploited in materials design [3, 11]. One of disadvantage of protein-based polymers is the limited number of building blocks, which are largely restricted to the 30 natural amino acids. Despite this limitation, protein-based polymers offer many advantages over traditional petro-polymers. The self-assembly of peptides provides a viable way to generate functional polymers. Second, biocompatible and biodegradable properties of these materials make them ideal for drug delivery vehicles and tissue engineering scaffolds.

1.2 Elastin-like Polypeptides

The sequence of elastin-like polypeptides is artificial, repetitive polypeptides derived from mammalian elastin. They are composed of pentapeptide repeats, Val-Pro-Gly-Xaa-Gly, where Xaa can be any amino acids except proline [4]. ELPs exhibit an inverse temperature transition behavior, which is they are soluble at temperatures below their transition temperature and become insoluble at temperature above it [5]. This process is fully reversible. The phase transition can be tuned at a molecular level by changing the guest residue composition and distribution, molecular weight, solution condition, etc.

This thesis is focused on the use of pH as a trigger of ELP phase transition behavior. Since pH plays a role in many biological processes, it can be used as trigger to develop bioresponsive therapeutics [11].

1.3 Inverse Temperature Transition

Protein-based polymers are stabilized by non-covalent intramolecular interactions between amino acids chains. Protein complexes are also formed by specific, non-covalent interactions [6]. All biological processes depend on proteins being stable and in the appropriate folded conformation. In general, the folding of and assembly of biological macromolecules from a random coiled chain to a well-organized structure represent a particular energy conversion. Change in chemical potential can give rise to the molecular organization of structure formation. Protein-based polymers, in which the hydrophobic (apolar) and polar residues are in the proper balance, will fold and assemble above a particular temperature and disassemble and unfold below this temperature [7]. This occurs by means of hydrophobic folding and assembly, i.e., the separation of oil-like moieties of the protein from water. The onset temperature of the transition is defined as T_t. This behavior of elastin-like polypeptides (ELP) is termed as an inverse temperature transition [5]. At the macroscopic level, this transition of ELP from soluble to insoluble by temperature stimuli can be observed easily. One means to determine this transition temperature is from temperature profiles by using UV-vis spectroscopy. The transition temperature is defined as the intersection of the tangent line of zero absorbance and the highest slope of the curve on a UV absorbance spectrum [8].

Based on the observation of this inverse temperature transition of ELPs, several studies have been done to explain the mechanism of this unique behavior. Yamaoka and Tamura`s work shows that the transition of ELP differs from the lower critical solution temperature (LCST) behavior of vinyl polymer [9], which thermoresponsiveness is rather independent of a wide range of polymer concentration [33]. They postulate the mechanism of ELP transition behavior is that when the temperature is increased, the peptides undergo a conformation change from more random chains into β-spiral structures [35] (Figure 1.1), exposing some hydrophobic groups to the aqueous solvent, resulting in a hydrophobic association [9].

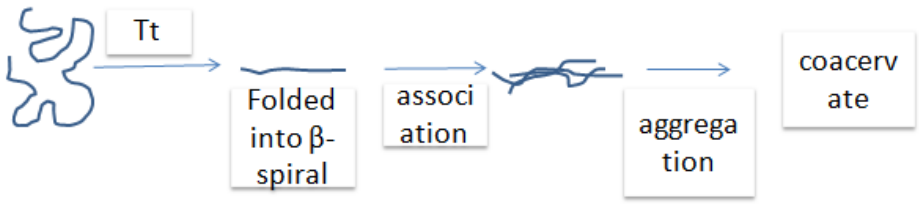

Figure 1.1: Mechanisms for phase transition for $(GVGVP)_n$ in an aqueous solution.

The transition temperature, T_t, is the temperature where the hydrophobic folding and assembly transition occur. At this point, the Gibbs free energy should be zero and we can write [5]:

$$T_t = \frac{\Delta H_t}{\Delta S_t}$$

T_t is a function of the differences in interactions of the water solvent and residues of ELPs. It can be used as a measure of the hydrophobicity of the residues as well as a measure of the number of waters of hydrophobic hydration that change to bulk water during hydrophobic folding [5].

1.4 Advantages of Elastin-like Polypeptide

Compared to traditional petro-polymers, one of outstanding advantages of ELPs is the inverse temperature transition, as described above. The responsive ability of ELPs is not restricted to temperature change; it can be controllably tuned by modifying the amino acid sequence of the polypeptides. Bulk hydrogels of ELP have been designed to respond to various external stimuli, like temperature or pH [10]. Also, genetic engineering allows scientists to obtain a complex and well-defined ELP with designed functions. Meanwhile, each molecule will have exactly same chain length, and the whole length could be up to 2000 or more residues [5]. Furthermore, the ELPs are stable over long periods of time in various conditions, since the side chain for the Gly (G), Val (V), and Pro (P) residues are either simply the hydrogen atom or an aliphatic grouping (Figure 1.2) [5].

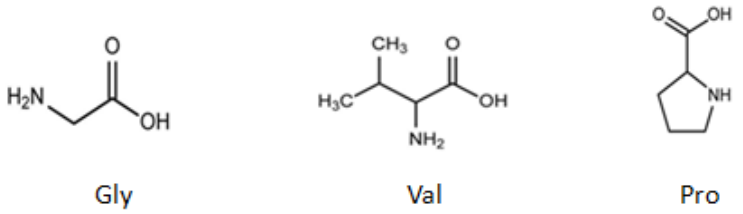

Figure 1.2: Chemical structures of Gly, Val, and Pro.

The basic composition when generating ELPs with amino acid substitutions is $(GVGVP)_{fy}(GXGVP)_{fx}$. Depending on the replaced residue X, stimulus triggering the phase transition could be various, irradiation [11], thermal and pressure. f_v is the molar fraction of (GVGVP), and f_x is the molar fraction of (GXGVP), where two molar fractions add up to 1. When acidic or basic amino acids are placed at some of the X

positions, the transition temperature of these ELPs becomes dependent on pH [41]. X in this work is glutamic acid, which has a carboxyl group (Figure 1.3). The carboxyl side chain would be fully ionized in a neutral aqueous condition.

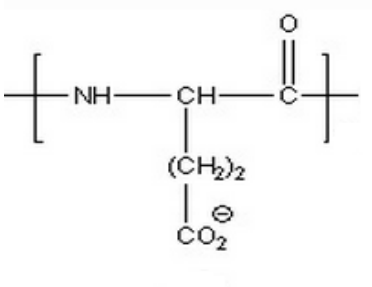

Figure 1.3: The chemical structure of carboxyl group.

The pH-responsive ELPs undergo a phase transition that can be isothermally triggered by a change in pH. The range of pH change is controlled by the type and number of ionized residues and the molecular weight of the ELP. It is possible to design a pH responsive ELP that responds to a specific range of pH which is optimal for the designed application.

Additionally, previous study has shown the biocompability of ELPs [39] by ASTM recommended generic biological tests [43]. The high segmental mobility of ELPs may help in preventing the identification of these foreign proteins by immune system [44].

1.5 Applications of ELPs

ELPs are useful for a wide variety of biomedical applications, due to their unique chemical and physical properties. First, the transition temperature, T_t, can be precisely

tuned between 0 and 100˚C. Second, ELPs can be synthesized as monodisperse polymers from genetic engineering, resulting in a precisely-defined molecular weight. The molecular weight is a key parameter for drug delivery, since it impacts both clearance from the body and half-life of polymer *in vivo* [11]. Third, biodegradable and biocompatibility of ELPs, as described in last section, suggests their suitability in biomedical applications.

ELPs have been used in drug delivery system [12], biosensors [13] flow controls in microfludic devices [14]. This section will discuss some current uses of ELPs in these fields.

1.5.1 ELPs used in drug delivery system

For pH and thermal responsive ELPs, the drug delivery system is a very interesting and promising field. Many works are leaning towards designing responsive drug carriers which can be stimulated by physiology stimuli, such as pH and temperature [16, 17]

The pH is a vital signal; there is a wide variation of physiological pH. For instance, along the gastrointestinal (GI) tract, pH value is from acidic in the stomach (pH=2) to basic in the intestine (pH=5-8) [15]. Ionisable polymers with a pK_a value between 3 and 10 are candidates for pH responsive system [18]. The carboxyl groups of glutamic acid are typically ionized in neutral and alkaline solutions; therefore ELPs would have a high transition temperature. The pH at which the pendant acidic groups become ionized depends on the ELP pK_a, which depends on the ELP composition. Also, the pK_a of ELPs can be shifted by positioning hydrophobic residues, phenylalanine for

example, beside the ionizable residues [5]. This is called hydrophobically induced pK_a shift, resulting in extraordinary pK_a towards higher values.

The pH and thermal responsive of ELPs led to a use as a drug carrier for cationic or anionic drugs. When charged residues of ELPs are complexed with an ionic, oppositely-charged drug, the T_t decreased dramatically. ELPs could have a lower T_t, which allows for transit at physiological temperature and entrapping the drugs. In previous studies, naltrexone, a cationic drug containing a tertiary amine (pK_a 9.4) was encapsulated with (GFGVPGEGVPGFGVP), which Glutamic acid (E) is an ionizable residue (pK_a 1.1) [1]. In the presence of naltrexone, T_t shifted from above 100˚C to 34˚C. This allows ELPs from insoluble aggregates release the drug slowly as it is leached from its coupling of the aggregates. As the drug is released from the ELP, the degree of coupling between the ELPs and the drug decreases and the interaction between drugs and ELPs is lost, resulting in the charged state of carboxyl group. At this point, T_t is much higher than the ambient temperature, ELPs unfold and dissolve.

1.5.2 ELPs used in tissue engineering

Biomaterials used in tissue engineering are required to fill and assume the shape of the replacement tissue, void or defect, support the cellular processes needed to regenerate tissue that will function like native tissue, provide physical properties for a given tissue, and remain fixed within the target area for a designed period of time [19-21].

ELPs are useful for tissue engineering due to their general biocompatibility. Secondly, ELPs themselves do not interact with encapsulated cells. So, ELPs can be

designed to be bioactive for specific needs [22]. Third, ELPs can be produced at a high level in *E. coil* (200-400 mg/L in shaker flask culture) [36]. Finally, ELPs can be easily purified by using inverse transition cycling without further processing, like chromatography [34].

ELPs can be crosslinked to form hydrogel networks. It has been shown that these hydrogels maintain contractile sensitivity to stimulus such as temperature [23]. Urry and his co-workers have formed ELP hydrogels through nonspecific radical cross-linking of ELPs in the coacervate state using γ -irradiation and have demonstrated preservation of the inverse phase transition [24]. Conticello and his co-workers showed that hydrogel could be fabricated from ELPs with engineered chemoselectivity for cross-link formation at precisely spaced periodicities along the peptide backbone [25]. The sequence for this kind of cross-linked hydrogel is $[(VPGVG)_4(VPGKG)]_n$, one lysine residue in every five pentapeptides. Crosslinking reagent used in the study was commercially available homobifunctional amine-reactive cross-linker. Moreover, they showed cross-linking in an organic solvent (typically DMF and DMSO), where ELP do not show inverse phase transition, leading to a more uniform structure.

1.6 Synthesis of Elastin-like Polypeptides

1.6.1 Chemical synthesis

Chemical synthesis is a traditional strategy to synthesize peptides. Chemical synthesis of the repeating peptides of elastin have been successful when the repeat units are relatively small, e.g., 3-9 residues [27]. When the desired polypeptides are more

complex, solid phase synthesis has been attempted with limited success. The reason is because of the difficulty of removing small amount of racemization in the purification process, and the small amount of errors can significantly alter the physical properties, like transition temperature, elastic moduli, etc. [48].

1.6.2 Genetic synthesis

Due to the development of molecular biology and gene manipulation, researchers have been able to design and synthesize almost any polypeptide sequences with high precision. A number of strategies have been designed to match these goals [49], but most of them are concatemerization of a monomer gene [50]. In this process, the double-strand monomer genes are generated either by enzyme digestion from original plasmid or by annealing of two complementary single-stranded DNA fragment. Then, monomer fragments are ligated to form oligomers of different length. Although concatemerization is rapid, it sacrifices precise control over the oligomerization process. It does not guarantee the synthesis of a gene with a desired length [1, 20].

ELPs are repetitive polypeptides, which require not only precise amino acid sequence, but specific molecular weight and composition. Therefore, a general strategy which is termed “recursive directional ligation” (RDL), is utilized to synthesis ELPs. This strategy was developed by Meyer and Chilkoti [29]. Figure 1.4 shows a schematic of RDL.

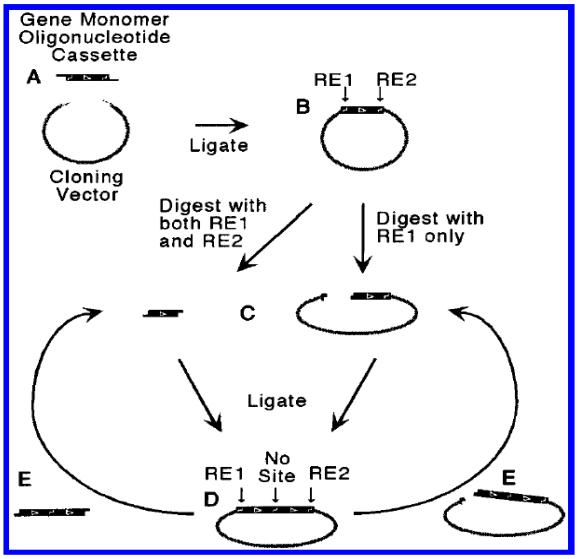

Figure 1.4: Overview of RDL (with permission from reference [29]). Copyright 2002 American Chemical Society.

Briefly, an oligomer was synthesized by annealing two single-stranded DNA fragments. The oligomers are designed so that two cohesive ends are on each end. Then vectors were linearized by restriction enzyme, resulting in two compatible cohesive ends with insert (A). Ligation was performed to produce a plasmid containing designed gene sequence (B). Two additional restriction endonuclease recognition sites are designed on each end of the coding sequence (RE1, RE2), internal to the initial two cut sites. To produce the vector for next cycle of dimerization, a single digestion with RE1 was performed. To produce compatible insert, double digestion with RE1 and RE2 was performed. The purified inserts then were ligated into purified vector, which double the size of gene monomer. Additional cycles could be performed, based on the length of designed coding sequence.

RDL are expected to achieve three goals by designing the monomer sequence:

1. The insert is ligated with its directionality preserved in a head-to-tail orientation upon ligation into vector.
2. The ligation is seamless; no extraneous residues are introduced at the ligation site.
3. Recognition site1&2 should remain at each end of the dimerized gene, no recognition sites are generated at the internal site of ligation.

1.6.3 Selection of RE1 and RE2

The selection of a pair of restriction endonucleases has to match four requirements:

1. Two RE must be different so that the DNA can be selectively cleaved either by one or by both of the enzymes and so that neither site is re-formed at the internal site of ligation.
2. Two enzymes must produce complementary, single-strand DNA overhangs upon cleavage.
3. At least one RE should be unique on the cloning vector so that digestion with enzyme cleaves the plasmid only at a single site.
4. The recognition sequence of two REs must be compatible with the coding sequence of the polypeptide.

For ELP synthesis, *Nde*I and *Bgl*I were selected as RE1 and RE2 on each end of monomer, respectively. The only difference is that we introduced *PflM*I between RE1 and RE2. Instead of single digestion, a double digestion with *Nde*I and *PflM*I was

performed to produce linearized vector. Figure 1.5 shows synthesis of the gene for ELP in our lab.

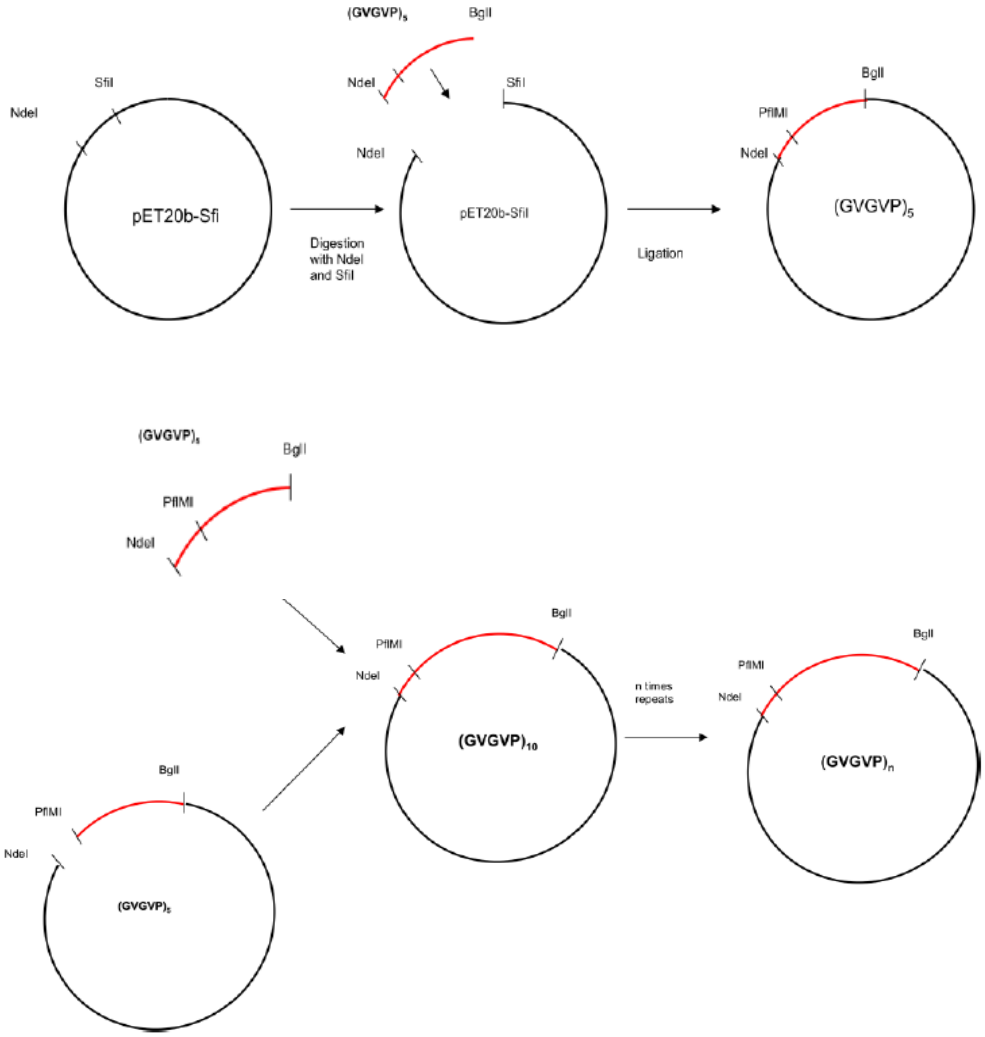

Figure 1.5: Schematic of RDL used in our lab to produce ELP gene.

*Nde*I and *Bgl*I have different recognition sequences, and thus meet the first requirement. Furthermore, the ends created by digestion with *PflM*I are compatible with those created by digestion with *Bgl*I, which meets the second requirement. Since there is no *PflM*I in cloning vector Pet20b, the *PflM*I recognition site we introduced on the vector

is unique, meeting the third requirement. The final requirement is the compatibility of these two enzymes with gene sequence, as illustrated in follow.

1. *Nde*I recognition sequence CA^TATG
2. *PflM*I recognition sequence CCANNNN^NTGG
3. *Bgl*I recognition sequence GCCNNNN^NGCC
4. Combined *PflM*I and *Bgl*I recognition sequence CCANNNN^ NGCC

To match the last requirement, a gene which has *Nde*I and *Bgl*I on each end and a *PflM*I recognition site at internal site was designed. 3' *Bgl*I recognition site on the gene combines with 5' *PflM*I recognition site on the cloning vector, as (4) showing above. 3' *Nde*I recognition site on the gene combines with 5' *Nde*I recognition site on the cloning vector. By designing recognition sites as mentioned above, the polypeptide repeat sequence is not disrupted at the site of ligation during RDL.

1.7 Foldon Domain

Bacteriophage T4 has a structural protein which contains a trimeric globular domain located at its C terminus [53]. This domain has been termed foldon [52] (Figure 1.6) [28]. This foldon domain is able to form an isolated trimeric foldon structure, which is stable at temperature of up to 75˚C [53]. Due to this extreme stability of the trimer, the foldon can be used as an artificial trimerization inducer or enhancer.

Figure 1.6: Ribbon diagram of the C-terminal foldon domain (with permission from reference [52]). Copyright 2004, Elsevier.

A previous study has shown that foldon domain was used as stabilization of short collagen-like triple helices by fusing peptides $(GPP)_{10}$ to the N-terminal of the foldon domain [54]. When fused to the folodn domain, trimer formation of $(GPP)_{10}$ is far less concentration dependent, and the onset temperature of the trimer unfolding is significant increased. These studies have inspired us to combine foldon domain to the ELPs in order to improve chemical and structural properties.

For linear ELP, transition temperature T_t is concentration dependent and generally shows an inverse-log dependence causing ELP in high concentration to transition at a lower T_t [55]. The linear ELPs fold into a β-spiral that is stabilized by a triple helix formed with two other identical polypeptides [26]. This triple helix formation is closely dependent on chain-chain interactions [27]. In other words, the ELP chains must diffuse to find other two chains to form a triple helix in the folding process. We proposed a new structure to which the ends of three ELP chains will be attached to the C-terminal foldon domain (Figure 1.7 A). In this new structure, the distance between ELP chains is

relatively short, so they do not need to diffuse a long distance at low concentration. Furthermore, this trimer structure is thermally stable up to 70˚C [54]. The ELP chains potentially could fold into triple helix stabilized β-spirals above T_t (Figure 1.7 B).

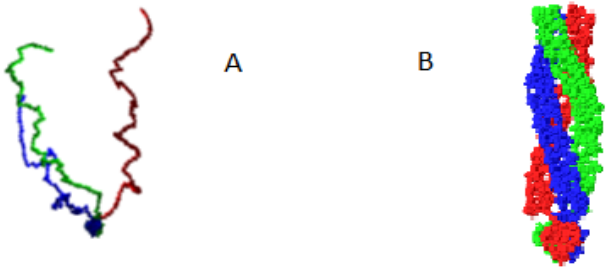

Figure 1.7: A. ELP-foldon is shown as an unfolded state below T_t. **B**. ELP-foldon is shown as a folded state above T_t [51].

1.8 Scope of the Thesis

This research is to better understand how the addition of the oligomerization domain (foldon) to a pH and thermally responsive ELP would alter its inverse transition behavior and to predict quantitatively the transition temperature of pH-responsive ELPs with two different structures by fitting our experimental data to a quantitative model.

In order to achieve this goal, two genes were designed and synthesized by utilizing recursive directional ligation (RDL). For ELP-foldon gene construct, a negatively charged trimer-forming foldon domain was incorporated at the ELP C-terminus. All constructs were expressed in *E. coli*.

The addition of the foldon domain is expected to control and improve the rate of ELP chains assembly as well as the pH and thermal transition behavior of the constructs. In order to illustrate the difference, we present experimental data of the transition

temperature of two different constructs measured as a function of concentration, a function of pH, and a function of salt (sodium chloride) concentration.

CHAPTER II

MATERIALS AND METHODS

In order to characterize pH and thermal responsive ELP, two different pH dependents ELPs were designed, expressed, and purified using standard techniques of molecular and microbiology. This section details all of the materials and methods. There were two main ELP constructs, $(GVGVPGEGVPGVGVP)_{n,}$ and $(GVGVPGEGVPGVGVP)_n$–foldon. The second construct has this oligomerization domain, named foldon, attached to its C terminal.

2.1 Synthesis of Genes

2.1.1 Synthesis of plasmid containing $(VEV)_{12}$ genes

The synthesis of $(VEV)_{12}$ follows the methods described by Meyer and Chilkoti [29]. The addition of foldon domain is inspired by Ghoorchian and Holland [31].

Cloning and expression were done in *E. coli* BL21* host strain by using the pET20b vector (Novagen). We started by designing complementary oligonucleotides (Invitrogen) that encoded MGH(GVGVPGEGVPGVGVP)G peptides with appropriate endonuclease recognition sites.

A thermal cycler was programmed to heat then slowly cool a 1:1 ratio of complementary oligonucleotides to form an annealed two-stranded VEV DNA. The reaction mixture contained two complementary oligonucleotides (4 µl, 97 nmol; 4 µl, 96 nmol; Life Technologies), 21 µl quick ligase buffer (New England BioLabs) and 21 µl nuclease free water (Promega). Initially, the mixture was heated to 95 ˚C for 5 minutes, then cooled down to 25 ˚C over 70 steps, then held at 4 ˚C for 55 minutes. The sequence of an annealed double stranded VEV (below) has sticky ends compatible with *Nde*I and *Bgl*I.

The annealed double stranded VEV DNA:

```
   M   G   H   G   V   G   V   P   G   E   G   V   P   G
T|ATG|GGC|CAC|GGC|GTG|GGT|GTT|CCG|GGG|GAA|GGT|GTA|CCA|GGT|G
   AG CCG GTG CCG CAC CCA CAA GGC CCC CTT CCA CAT GGT CCA|C


V   G   V   P   G
TG|GGA|GTG|CCG|GGC
AC CCT CAC GGC
```

The annealed VEV was ligated into a linearized pET20b cloning vector. The cloning vector was first prepared by modifying the DNA sequence spanning *Nde*I to *Eco*RI of pET20b by cassette mutagenesis to incorporate a unique *Sfi*I recognition site.

The modified pET20b, termed pET20b-*Sfi*I (shown below), was double digested by *Nde*I and *Sfi*I, removing the highlighted portion.

pET20b-*Sfi*I cloning region:

```
   NdeI                              SfiI                        EcoRI
    M    S    K    G    P    G    W    P   ter  ter
T ATG AGC AAA GGG CCG GGC TGG CCG TGA TAA
A TAC TCG TTT CCC GGC CCG ACC GGC AGT ATT
```

Restriction endonuclease *Sfi*I recognizes interrupted palindromic sequence 5' – GGCCNNNN^NGGCC- 3' (N can be any base, ^ indicates the cut-site). *Bgl*I recognizes the interrupted palindromic sequence 5'-GCCNNNN^NGGC-3'. Therefore, the *Bgl*I cut DNA can have a compatible end with *Sfi*I cut DNA, allowing ligation between pET20b-*Sfi*I vector and VEV insert [32].

The double digestion protocol of pET20b-*Sfi*I is as follows:

- pET20b- *Sfi*I DNA 15 µl
- NEB 10x Buffer 4 4 µl
- *Nde*I restriction enzyme 2 µl
- *Sfi*I restriction enzyme 2 µl
- Nuclease Free Water 17 µl

All the components were mixed thoroughly in a 1.5 ml microcentrifuge tube. Then this solution was incubated in a 37 ˚C water bath for 3 hours, after which it was run

on a 2% agarose gel in TAE buffer (40 mM Tris acetate, 2 mM EDTA, pH 8.5) at 80 V. The sample was mixed with 6x loading dye (Promega) to a volume of 48 µl. A 100 base pair DNA ladder was used to identify the appropriate band to excise. The gel slice was weighed and purified by using a DNA extraction kit (Genscript). The final DNA vector was eluted in EB buffer (Tris-Cl, pH 8.5).

The ligation procedure was done using a Quick Ligation Kit (NEB), combining the vector and insert solution in a volume ratio of 1:3. The total volume of ligase mixture was 20 µl with 10 µl being used for transformation (described below) and the rest stored at -20 ˚C.

- Thaw chemically competent *E. coli* cells on ice.
- Chill 10 µl of the ligation mixture on ice
- Add 50 µl competent cells to ligation mixture and mix gently by pipetting up and down, then chill on ice for 30 minutes.
- Heat shock for 2 minutes at 37 ˚C, then chill on ice for 5 minutes.
- Add 950 µl room temperature LB medium without ampicillin, incubate in water bath for one hour at 37 ˚C
- Spread 300 µl of transformation mixture onto LB agar plates with ampicillin.
- Incubate overnight at 37 ˚C.

After overnight incubation, colonies were picked from the agar plates, and grown in a 5 ml LB medium with ampicillin. The cultures were incubated at 37 ˚C and shaken at 300 RPM overnight. A QIAGEN Plasmid Mini-Prep Kit was used to purify the DNA.

Before the mini-prep, frozen stocks for long-term storage were made by mixing 400 µl 50% glycerol with 500 µl cell cultures.

In order to verify that the purified plasmid had the appropriate length DNA ligated, PCR was run to amplify the designed DNA sequence (see protocol below). The products were run on a 2% agarose gel with TAE buffer for screening. A control gene sequence was made from pET20b- *Sfi*I by using the same method. Gene length of control sample and designed products are 239 base pair and 278 base pair, respectively.

PCR protocol:

- PCR Master Mix 12.5 µl
- T7 forward primer 2.5 µl
- T7 reverse primer 2.5 µl
- DNA 1 µl
- Nuclease Free Water 6.5µl

The T7 Forward and T7 Terminator primers (Invitrogen Inc.), which are complementary to the 3' ends of the target DNA segment of interest, were used in the PCR reaction.

T7 Forward:

5' TAA TAC GAC TCA CTA TAG G 3'

T7 Terminator:

5'GCT AGT TAT TCG TCA GCG G 3'

The pET20b containing the gene of (VEV) served as a vector for the next round of cloning. The vector was linearized with enzymes *Nde*I and *Pflm*I.

- pET20b(VEV) DNA 15 µl
- Buffer 2 4 µl
- *Nde*I restriction enzyme 2 µl
- *Pflm*I restriction enzyme 2 µl
- Nuclease Free Water 17 µl

All of the components were mixed thoroughly, and then incubated at 37 ˚C for 3 hours. After incubation, linearized vectors were separated by running on a 2% agarose gel in TAE buffer. The gel slice was cut based on the molecular weight of the vector; QIAGEN quick Gel Extraction Kit was used to purify the vector.

Ligation, transformation and DNA mini-prep were performed to obtain pET20b $(VEV)_2$. PCR reactions were run in the thermal cycler to amplify (VEV) and $(VEV)_2$. Screening on the agarose gel confirmed the size of $(VEV)_2$. One more cycle was performed in order to obtain pET20b $(VEV)_3$. After pre-screening, pET20b $(VEV)_3$ was sent for DNA sequencing. The DNA sequencing was carried out with T7 primer at the Cleveland Clinic Foundation Genomics Core Facility.

At this point we use the previous products pET20b-$(VEV)_n$ as starting materials for next round cloning process, resulting in a pET20b-$(VEV)_{2n}$. Linearization of vector was exactly the same as described above. $(VEV)_n$ inserts were made by double digesting pET20b-$(VEV)_n$ with *Nde*I and *Bgl*I.

- pET20b-$(VEV)_n$ DNA 15 µl
- Buffer 2 4 µl
- Nuclease Free Water 16.6 µl
- Bovine Serum Albumin 0.4 µl
- *Nde*I restriction enzyme 2 µl
- *Bgl*I restriction enzyme 2 µl

The double digestion solution was incubated in a 37 ºC water bath for 3 hours, then run on a 2% agarose gel in TAE buffer at 80 V. Excision of the gel slice was based on the size of the designed DNA length. Purification of the gel slice and ligation and transformation of the purified $(VEV)_n$ insert and vector were done as described above. The cloning process was repeated until the designed gene, $(VEV)_{12}$, was obtained.

2.2 Protein Expression and Purification

Protein expression and purification follows the method described by Meyer and Urry [34, 36].

2.2.1 Expression

The pET20b expression vectors containing ELP genes were transformed into the *E. coil* BL* host strain for expression. The procedure started with preparation of growth medium and starter cultures. Luria-Bertani (LB) media was used as growth medium. To prepare the media, sodium chloride (5 g), yeast extract (5 g), Peptone (10 g) were mixed with 1 L distilled water in a 2 L Erlenmeyer flask and autoclaved.

For each expression, a starter culture was made by transferring transformed cells from frozen stocks (-70 ºC) into 10 ml LB media with ampicillin (0.1 g/L). The culture was incubated at 37 ºC with shaking (300 RPM). After overnight growth, ampicillin (0.1 g/L) was added to LB media, and the 1 L media was incubated with the starter culture. Expression cultures were incubated with shaking (300 RPM) at 37 ºC. When OD_{600} reached 0.8-1.0, the culture was induced by the addition of IPTG (1 mM) [29]. The cells were harvested 4 hours after induction by cold centrifuge at 8000-9000 xg for 20 -25 min at 4 ºC. The cell pellets were kept at -20 ºC for short-term storage.

To determine how well ELPs were expressed by *E. coil* host strain and the location of ELPs (soluble or insoluble phase) for purification, 1mL samples were taken from expression media over time (before induction, 2 hours after induction, and 4 hours after induction, and right before purification). These expression samples were spun down in a table-top centrifuge at 13000 xg for 5 minutes. Supernatants were discarded immediately; bacterial pellets were stored at -20 ºC in order to later perform mini-scale bacterial protein extraction and protein gel analysis.

2.2.2 Purification

ELPs were purified by inverse transition cycling (ITC) [7, 8]. During the purification procedure, the protein solution was selectively separated from other contaminants by heating up or cooling down repeatedly, with supplementing NaCl and acetic acid.

The frozen cell pellets were taken out from the freezer, and kept at room temperature for 15 minutes. Then cell pellets were resuspended in 30 ml of cold

phosphate buffered saline, PBS, then transferred to a 50 ml falcon tube, and lysed by sonic disruption at 4 ºC, with 90 s of sonication at maximum power, using 10s pulses separated by 20 s (550 Sonic Dismembrator, Fisher Scientific). After sonication, cell lysate was transferred to a centrifuge tube, and 1 M acetic acid was added to obtain a pH of 3.5-4. Salt, (2 M NaCl) was also added. The acid and NaCl lower the transition temperature of ELPs [4, 5]. The cell lysate was centrifuged at 13000 xg for 20 min at 4 ºC to remove insoluble cellular matter. The supernatant was removed and then heated up above the ELP transition temperature for 45 to 60 minutes. The aggregated ELP was separated from solution by centrifugation at 14000 xg, for 25 minutes at 40 ºC. The supernatant, containing soluble contaminants from the lysed *E. coil* cells was removed immediately and discarded. The protein pellet was put on ice and resuspended in 5 ml PBS. Once fully resuspended, the protein solution was centrifuged at 13000 xg, for 20-25 minutes at 4 ºC to remove the insoluble contaminants. After the cold centrifugation, the supernatant was transferred to another tube and the first round of inverse transition cycling is complete.

Typically, two rounds of inverse cycling were performed sequentially to purify the ELP. The addition of acetic acid and NaCl before hot incubation was the same as described above. After final cold centrifugation, the ELP was in 5 mL PBS. When properly purified, the solution was clear and transparent below T_t.

2.3 Protein Characterization

2.3.1 SDS-PAGE gel

The purified ELPs were first characterized by using 10-20% gradient Tris-Glycerol SDS-PAGE (Lonza) to confirm the purity and molecular weight [38]. The samples (typically 15 µl) were prepared in loading buffer containing 0.1% SDS and heated at 100 ºC for 5 minutes. Boiled sample were loaded on the gel at room temperature. For ELP-foldon samples, we also ran a non-boiled protein samples to verify the formation of trimer structure. The SDS-PAGE gels were later visualized by staining with GelCode blue stain reagents (Thermo).

2.3.2 Measurement of protein concentration

The method and extinction coefficients used in this measurement is based on Gill and Von Hippel's work [41]. This method provides accurate (+/-5% in most cases) molar extinction coefficients for protein at 280 nm, simply from knowledge of the amino acid composition. In this method, the proteins are required to be at the denatured state. For ELPs, under their expected transition temperature, they are random coiled chain in solution. Therefore, ELP solution can be measured directly without other processes. Table 2.1 gives molar extinction coefficient of model compounds.

Table 2.1: Values of the Molar Extinction Coefficients at 280 nm. Extinction coefficients are in units of $M^{-1}cm^{-1}$ [41].

Model compound	Extinction coefficient at 280 nm
N-Acetyl-tryptophanamide	5690
Gly-L-Tyr-Gly	1280
Cystine	120

Using these data, the extinction coefficient of a denatured protein can be calculated by using

$$\epsilon_{M,denatured} = a\epsilon_{M,Tyr} + b\epsilon_{M,Trp} + c\epsilon_{M,Crs}\,, \quad [45]$$

where $\epsilon_{M,Tyr}, \epsilon_{M,Trp}$ and $\epsilon_{M,Crs}$ are the molar extinction coefficients of tyrosine, tryptophan, and cysteine residues at 280 nm (Table 2.1); a, b and c are the number of each residue in one protein molecule.

The concentration of proteins was quantified by using UV absorption at 280 nm on a Biomate3 (Thermo Scientific). First, a blank was measured with 1ml PBS, then 5% protein solution was made by mixing 50 µl protein sample with 950 µl PBS. Second, the absorption of the protein solution was measured. At this point, Beer`s law is used to calculate the protein concentration:

$$C_{denatured\ protein} = \frac{A_{denatured\ protein}}{\epsilon_{denatured}}\,, \quad [46]$$

$A_{denatured\ protein}$ is the measured optical density of the sample, and $\epsilon_{denatured}$ is the molar concentration of the denatured protein in the solution. For $(VEV)_{12}$, each molecule only has one tryptophan residue, giving a value of the extinction coefficient of 5690

M^1cm^{-1}; for $(VEV)_{12}$ –foldon, each molecule has two tyrosine and two tryptophan, giving a value of extinction coefficient of 13940 $M^{-1}cm^{-1}$. With knowing these data, the concentration of a known amino acids sequence of protein can be easily calculated.

2.3.3 Thermal Characterization

To characterize inverse transition temperature of ELP and ELP- foldon, the OD_{350} of ELP solution was monitored as a function of temperature on a Cary UV-Visible spectrophotometer [29]. The heating and cooling rate was 0.5 $^oC\ min^{-1}$. The ELP sample (typically 2 ml) was loaded in a 10 mm path length quartz cuvette. A small stir bar was placed in the cuvette to perturb the sample. The derivative of the turbidity profile with respect to temperature at 350 nm was numerically calculated, and the onset temperature, T_t is defined as the intersection between tangent of zero absorbance and the maximum slope on the temperature versus absorbance curve [47].

This transition temperature measurement was performed on two ELPs: $(VEV)_{12}$ and $(VEV)_{12}$-foldon. Transition temperature was also measured as a function of concentration, pH, and NaCl concentration.

CHAPTER III

RESULTS AND DISCUSSION

3.1 Preparation of Polypeptides

3.1.1 Design and synthesis of genes synthesis

The genes for $(VEV)_{12}$ and $(VEV)_{12}$-foldom were successfully made. Samples of the plasmids containing these products were sequenced at Cleveland Clinic Foundation and the results for the products as well as some precursors are provided below.

DNA sequence of pET20b $(VEV)_3$:

*Nde*I *Pflm*I

TATGGGCCACGGCGTGGGTGTTCCGGGGGAAGGTGTACCAGGTGTGGGAGTGCCGGGCG

TGGGTGTTCCGGGGGAAGGTGTACCAGGTGTGGGAGTGCCGGGCGTGGGTGTTCCGGGG

GAAGGTGTACCAGGTGTGGGAGTGCCGGGCGTGGGTGTTCCGGGGGAAGGTGTACCAGG

TGTGGGAGTGCCGGGCGTGGGTGTTCCGGGGGAAGGTGTACCAGGTGTGGGAGTGCCGG

GCGTGGGTGTTCCGGGGGAAGGTGTACCAGGTGTGGGAGTGCCGGGCTGGCCG

BglI

Translated sequences to protein of pET20b $(VEV)_3$:

GHGVGVPGEGVPGVGVPGVGVPGEGVPGVGVPGVGVPGEGVPGVGVPGVGVPGEGVPGV

GVPGVGVPGEGVPGVGVPGVGVPGEGVPGVGVPGWP

DNA sequence of pET20b $(VEV)_{12}$:

*Nde*I *Pfl*I

TATGGGCCACGGCGTGGGTGTTCCGGGGGAAGGTGTACCAGGTGTGGGAGTGCCGGGCG

TGGGTGTTCCGGGGGAAGGTGTACCAGGTGTGGGAGTGCCGGGCGTGGGTGTTCCGGGG

GAAGGTGTACCAGGTGTGGGAGTGCCGGGCGTGGGTGTTCCGGGGGAAGGTGTACCAGG

TGTGGGAGTGCCGGGCGTGGGTGTTCCGGGGGAAGGTGTACCAGGTGTGGGAGTGCCGG

GCGTGGGTGTTCCGGGGGAAGGTGTACCAGGTGTGGGAGTGCCGGGCGTGGGTGTTCCG

GGGGAAGGTGTACCAGGTGTGGGAGTGCCGGGCGTGGGTGTTCCGGGGGAAGGTGTACC

AGGTGTGGGAGTGCCGGGCGTGGGTGTTCCGGGGGAAGGTGTACCAGGTGTGGGAGTGC

CGGGCGTGGGTGTTCCGGGGGAAGGTGTACCAGGTGTGGGAGTGCCGGGCGTGGGTGTT

CCGGGGGAAGGTGTACCAGGTGTGGGAGTGCCGGGCGTGGGTGTTCCGGGGGAAGGTGT

ACCAGGTGTGGGAGTGCCGGGCTGGCCG

*Bgl*I

Translated sequences to protein of pET20b-$(VEV)_{12}$:

MGH$(GVGVPGEGVPGVGVP)_{12}$GWP

For the pET20b $(VEV)_{12}$-foldon, the encoded amino acid sequence is as follows:

Translated sequences to protein of pET20b $(VEV)_3$:

MGHGVGVPGEGVPGVGVPGVGVPGEGVPGVGVPGVGVPGEGVPGVGVPGVGVPGEGVPG

VGVPGVGVPGEGVPGVGVPGVGVPGEGVPGVGVPGWP

DNA sequence of pET20b $(VEV)_{12}$:

*Nde*I *Pflm*I

TATGGGCCACGGCGTGGGTGTTCCGGGGGAAGGTGTACCAGGTGTGGGAGTGCCGGGCG

TGGGTGTTCCGGGGGAAGGTGTACCAGGTGTGGGAGTGCCGGGCGTGGGTGTTCCGGGG

GAAGGTGTACCAGGTGTGGGAGTGCCGGGCGTGGGTGTTCCGGGGGAAGGTGTACCAGG

TGTGGGAGTGCCGGGCGTGGGTGTTCCGGGGGAAGGTGTACCAGGTGTGGGAGTGCCGG

GCGTGGGTGTTCCGGGGGAAGGTGTACCAGGTGTGGGAGTGCCGGGCGTGGGTGTTCCG

GGGGAAGGTGTACCAGGTGTGGGAGTGCCGGGCGTGGGTGTTCCGGGGGAAGGTGTACC

AGGTGTGGGAGTGCCGGGCGTGGGTGTTCCGGGGGAAGGTGTACCAGGTGTGGGAGTGC

CGGGCGTGGGTGTTCCGGGGGAAGGTGTACCAGGTGTGGGAGTGCCGGGCGTGGGTGTT

CCGGGGGAAGGTGTACCAGGTGTGGGAGTGCCGGGCGTGGGTGTTCCGGGGGAAGGTGT

ACCAGGTGTGGGAGTGCCGGGCTGGCCG

*Bgl*I

Translated sequences to protein of pET20b-$(VEV)_{12}$:

MGH(GVGVPGEGVPGVGVP)$_{12}$GWP

For the pET20b $(VEV)_{12}$-foldon, the encoded amino acid sequence is as follows:

Protein Translated from this Sequence $(VEV)_{12}$-foldon:

MGHGVGVPGEGVPGVGVPGVGVPGEGVPGVGVPGVGVPGEGVPGVGVPGVGVPGEGVPG
VGVPGVGVPGEGVPGVGVPGVGVPGEGVPGVGVPGVGVPGEGVPGVGVPGVGVPGEGVP
GVGVPGVGVPGEGVPGVGVPGVGVPGEGVPGVGVPGVGVPGEGVPGVGVPGWPGYIPEA
PRDGQAYVRKDGEWVLLSTFL

3.1.2 Expression and purification of linear $(VEV)_{12}$

In order to track expression process of ELPs, pre-induction and post-induction samples were taken from expression lysate. Then mini-scale protein extraction method was performed to isolate the protein in order to determine the location of proteins. Figure 3.1 presents the expression of $(VEV)_{12}$ in BL21* and final purified proteins. The molecular weight of $(VEV)_{12}$ is expected to be 15119.6 Da, as calculated based on the amino acid sequence, using a protein molecular weight calculator provided from protein information resource [47].

Sodium dodecyl sulfate polyacrylamide gel electrophoresis (SDS-PAGE) was used to confirm the size and purity of expression samples and purified proteins. By using this analysis method, trimer formation in $(VEV)_{12}$-foldon was verified and thermal stability of $(VEV)_{12}$-foldon sample was determined.

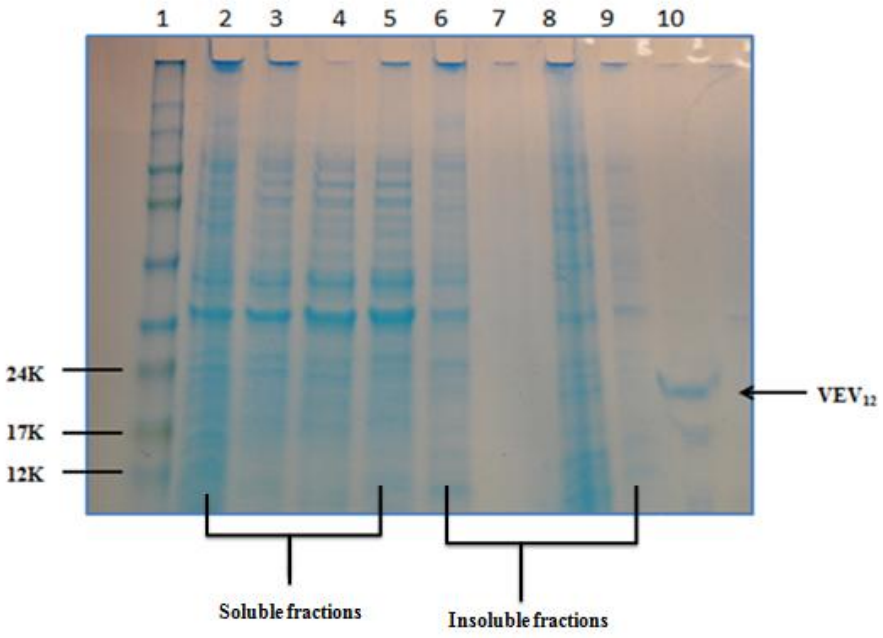

Figure 3.1: SDS-PAGE gel from $(VEV)_{12}$ expression process, and final protein. Lane 1 is the full range molecular weight marker (GE healthcare), ranging from 12 kD-225 kD. Lane 2 to lane 5 are soluble fractions, Lane 2 is right before induction, lane 3 to lane 5 are taken after induction, at 1h, 2h and 5h. Lane 6 to lane 9 are insoluble fractions, arranged in the same order. Lane 10 is purified VEV_{12}.

From the gel, the overexpressed polypeptides were accumulating in solution fraction over time. Those samples showed up around 18 kD, which is close to the calculated molecular weight of $(VEV)_{12,}$ 15 kD.

3.1.3 Expression and purification of $(VEV)_{12}$-foldon

Samples of VEV_{12}-foldon were taken during expression and extracted in the same manner as VEV_{12}. Molecular weight of VEV_{12}-foldon is 19 kD, based on calculation from the amino acid sequence.

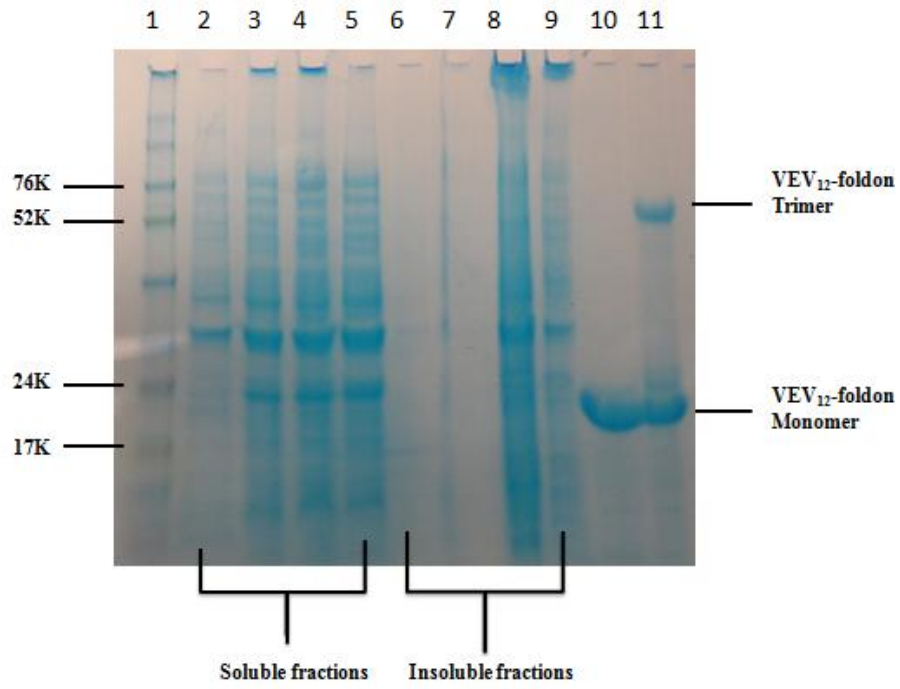

Figure 3.2: SDS-PAGE gel of $(VEV)_{12}$-foldon expression process and purified proteins. Lane 1 is the full range molecular weight marker (GE healthcare), ranging from 12 kD-225 kD. Lane 2 to lane 5 are soluble fractions, with lane 2 is right before induction, lane 3 to lane 5 are samples taken after induction, at 1h, 2h and 5h. Lane 6 to 9 are insoluble fractions arranged in the same order. Lane 10 is the boiled protein; lane 11 is the non-boiled protein.

The final purified VEV_{12}-foldon, boiled and non-boiled, were compared using SDS-PAGE (Figure 3.2, lane 10 and 11, respectively). The boiled sample follows the normal procedure where the protein solution is held for five minutes at 100 ˚C, which is well above the thermal stability temperature of the foldon domain [54]. Under these conditions, trimers are expected to be disrupted into monomers, resulting in a band at 19 kD. Non-boiled sample is loaded without heating, working to illustrate trimer formation. The foldon self-assembles into a trimer with three ELP chains attached to its C-termini. As indicated on the gel, a band shows up around 60 kD, which is about 3 times higher than the monomers. An interesting observation from the gel is that the non-boiled sample has a large fraction of monomers. This phenomenon may caused by the fact that our ELPs are ionic at the loading condition, which repulsive force may have effect on trimer formation.

The gel results shown above confirmed that both linear and trimer ELPs have been successfully expressed and purified, and a typical yield from expression is 20 mg/L.

3.2 Transition Temperature Determination

The transition temperature of ELP (T_t) is defined as the temperature where ELPs associate and aggregate, leading to a turbid solution. UV absorption at wavelengths 350nm as a function of temperature is measured in a UV-Visible spectrometer to determine T_t. For high molecular weight ELP or at high ELP concentrations, the transition is rather sharp, and also originally was defined as the temperature at the mid-point between the baseline and maximum in the curve [47]. However, for low

concentration samples, the slope of the turbidity curve is significantly smaller, and so cloud point determination has been shown to more accurately represent T_t. This method (Figure 3.3) was used to measure T_t in this thesis.

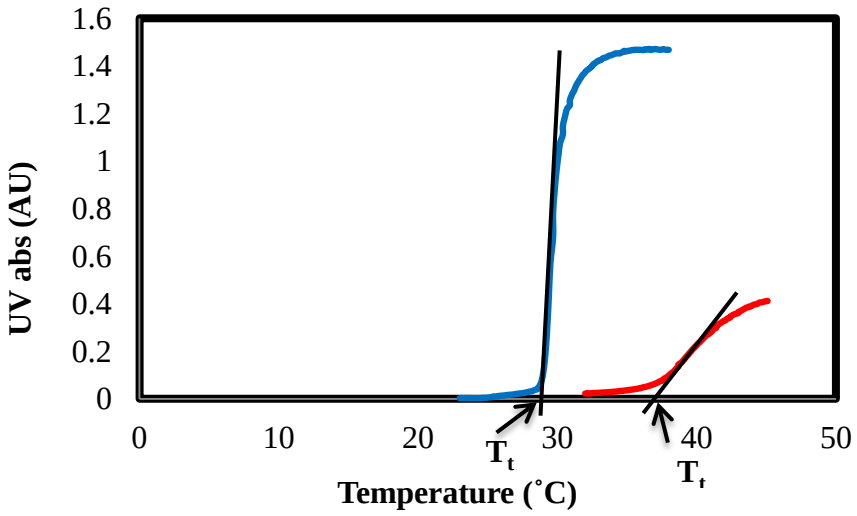

Figure 3.3: UV absorbance of VEV_{12}-foldon at high and low concentrations. Samples were heated at a rate of 0.5˚C/min. As shown in the figure, the high concentration sample has a shaper curve. For low concentration sample, the maximum slope of the curve is smaller. T_t is determined by the intersection between a tangent line of the point of maximum slope on curve and zero absorbance line.

3.3 T_t as a Function of Concentration

With the goal of quantitatively predicting the T_t of pH-responsive ELPs, T_t values for $(VEV)_{12}$ and $(VEV)_{12}$-foldon were determined for solutions of varying ELP

concentration. Previous studies have shown that, transition temperatures decrease for increasing concentration of ELP solution and increasing molecular weight [5, 25]. The phase transition behavior of $(VEV)_{12}$ and $(VEV)_{12}$-foldon should also be affected by the pH value of solution, due to the ionizable residue, glutamic acids [5]. When pH of solution is above pK_a of such ionizable residues, they are partially or fully deprotonated, resulting in a charged ELP with a higher transition temperature [5]. When below pK_a, the groups are protonated, leading to a much lower transition temperature. To illustrate this effect, T_t as a function of concentration was measured at two different pH values.

The transition temperatures for different concentrations were first measured at pH 2.7 (Figure 3.4), where $(VEV)_{12}$ and $(VEV)_{12}$-folodon should be fully protonated. The concentration range for linear ELPs is between 5 μM and 200 μM. The molar concentration of the trimer is one third of the concentration of the ELP-foldon monomers, since three ELP-foldon monomers self-assemble into a trimer structure in a aqueous solution. As is expected [59, 60], the data also show that T_t is lower for trimer ELPs compared to linear ones at the same concentration.

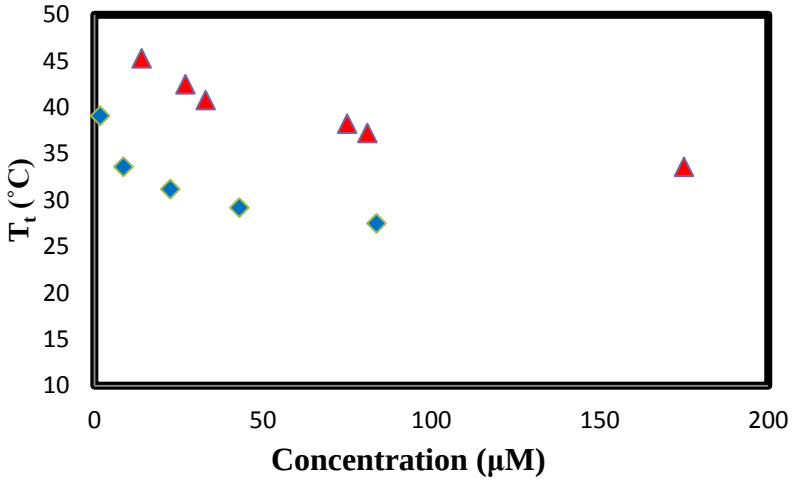

Figure 3.4: $(VEV)_{12}$ and $(VEV)_{12}$-foldon transition temperature as a function of ELP concentration at pH2.7, where both linear (triangle) and trimer (diamond) ELPs are expected to be fully protonated.

As mentioned above, the T_t value for linear and trimer ELPs are expected to increase as pH increases, due to ionizable residues along ELP chains. To show this, T_t as a function of concentration was measured at pH 3.8 and pH 4.2 for linear and trimer ELPs, respectively (Figure 3.5).

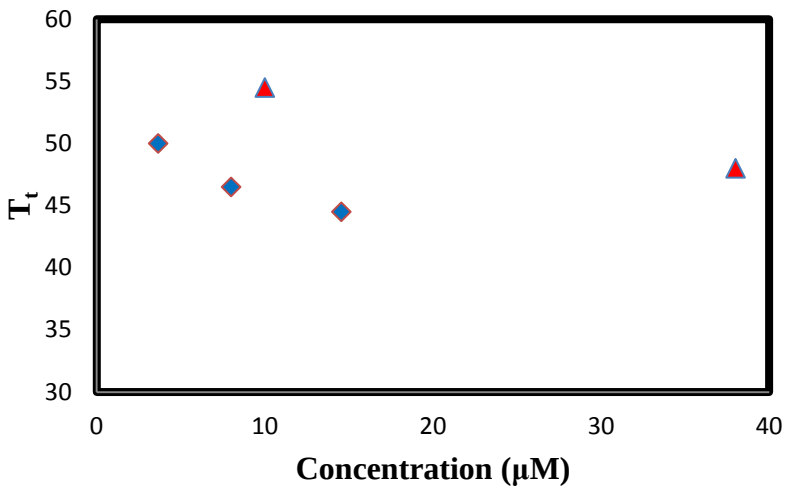

Figure 3.5: T_t of $(VEV)_{12}$ (triangle) as a function of concentration at pH 3.8. T_t of $(VEV)_{12}$ –foldon (diamond) as a function of concentration at pH 4.2.

3.4 Modeling the Transition Temperature

3.4.1 Model of pH effect on T_t

Our experiment shows that besides concentration, solution pH and molecular configuration of ELPs also have an effect on T_t. In order to describe the effect of pH and configuration on the phase transition temperature, a modified model was introduced to predict T_t as a function of concentration, and pH [64].

Based on Urry's phase diagram [5], Meyer and Chilkoti developed a model to describe how concentration and length of different linear ELPs affects their T_t [55].

$$T_t = T_{cr} + \frac{K}{L} \ln \left[\frac{C_{cr}}{C}\right] \qquad (1)$$

where the T_t for all length converge at the critical transition temperature (T_{cr}), and critical molar concentration (C_{cr}), L is the number of pentapeptide repeats, K is a parameter for length-concentration dependence interaction with a unit of ˚C. In protonated state, data for both linear and trimer ELPs show that T_t is a function of the log of ELP concentration as predicted by the model (Figure 3.6).

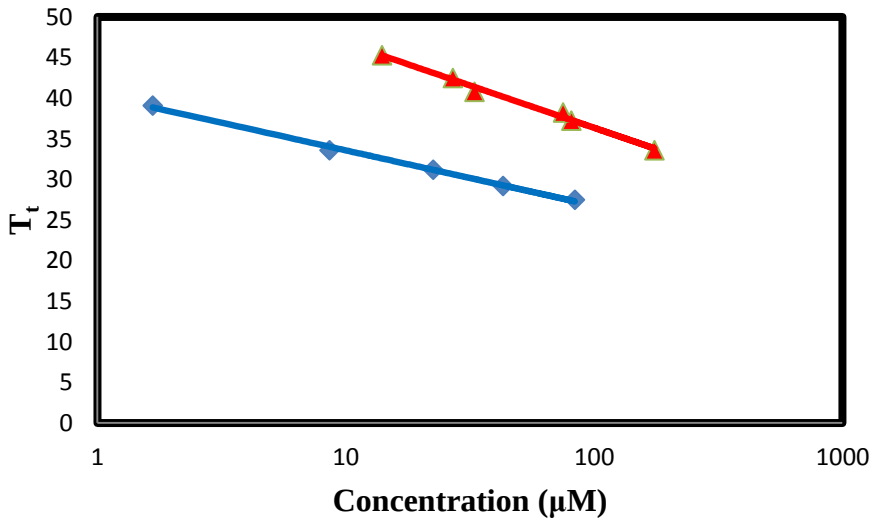

Figure 3.6: Transition temperature versus log concentration for linear (triangle) and trimer (diamond) ELPs. Our experimental data for linear and trimer ELPs fits in the Meyer and Chiilkoti model [55] very well.

3.4.2 Determination of critical point of linear and trimer ELPs

In Meyer`s model, the critical point, defined as C_{cr} and T_{cr} values, is empirically determined, which requires transition temperature of at least two different chain lengths

to be measured. However, only one construct of $(VEV)_n$ and $(VEV)_n$-foldon were made in this work. In order to overcome this limitation, it has been demonstrated that [51] using volume concentration (C_v) instead of molar concentration (Equation 2), T_{cr} is consistent with the T_t value predicted by the amino acid side chain hydrophobicity reported by Urry [5].

$$T_t = T_{cr} + \frac{K}{L}\ln\left[\frac{C_{Vcr}}{C_V}\right] \qquad (2)$$

Using the known T_{cr} value in this model allows for the determination of C_{cr} with the measurement of only one chain length. Below the transition temperature, ELPs are random coil in aqueous solution. The volume of random coil is equivalent to hydrodynamic volume, V_e, which is related to the average polymer conformation, indicating the geometry of the coil and the degree of swelling. For a given molecular concentration, C_m, there is a scaling relationship allowing conversion to volume concentration, C_v [30].

$$C_V = C_m L^n k' \qquad (3)$$

where k' is a scaling parameter. At critical point, $C_{cr,v}$ is defined to be 1, where the total volume of polymer coil is equal to the solution volume [51]. For $(VEV)_n$, the value of n is assumed to be 1.5, which is the predicted value for a linear polymer in a random coils [51].

The T_{cr} that used in volume concentration model is from T_t based hydrophobic scale developed by Urry [5], since those reported data have a good agreement with volume concentration model [51]. Urry produced this scale based on the observation of a linear relationship between transition temperature and molar fraction of amino acid substitution f_x, where X is a guest residue in $(GXGVP)_n$ [5]. The reported T_t of protonated $(GEGVP)_n$ is 30 ˚C, and the reported T_t of $(GVGVP)_n$ is 24 ˚[5]. For f_E = 1/3, the predicted T_{cr} of $(VEV)_{12}$ is 26 ˚C.

Combining Equations 3 and 4, we can write:

$$T_t = T_{cr} + \frac{Kpro}{L} \ln \left[\frac{1}{C_m L^n k`}\right] \qquad (4)$$

Experimental data of T_t versus [C] in protonated state was fit into Equation 4 to determine K_{pro} and k' (Table 3.1). For ELPs with two different chain lengths, we can write:

$$T_{t1} = T_{cr} + \frac{Kpro}{L_1} \ln \left[\frac{1}{C_m L_1^n k`}\right] \qquad (5)$$

$$T_{t2} = T_{cr} + \frac{Kpro}{L_2} \ln \left[\frac{1}{C_m L_2^n k`}\right] \qquad (6)$$

At the critical point, ELPs have the same T_t, giving the molar critical concentration, $C_{cr,m}$:

$$C_{cr,m} = e^A, \qquad (7)$$

where A = $\frac{n(L_2 lnL_1 - L_1 lnL_2)}{L_1 - L_2}$ - $lnk`$

Similar calculation was carried out for trimer ELP in protonated state. The only difference is the scaling parameter *n*. For trimer ELPs, *n* is equal to 2.3 [51]. Using the

critical molar concentration, equation 1can be used to calculate the T_{cr} for the molar concentration model. This allows us to predict T_t of linear and trimer ELPs as a function of concentration in protonated state.

Table 3.1: Multiple parameters describing the dependence of the transition temperature on concentration at protonated state

ELPs	pK_a	$T_{cr,\,pro}$ (˚C)	K_{pro} (˚C)	C_{cr} (μM)	$\boldsymbol{k}$` (L.mol^{n-1}.gr^{-n})	n
$(VEV)_{12}$	4.8	19.2	163	4312	4.7	1.5
$(VEV)_{12}$-foldon	4.8	18.2	365	1158	0.18	2.3

3.4.3 Effect of pH on Transition Temperature Modeling

As mentioned above, pH value in solution has a significant impact on T_t of acidic ELPs. To describe this effect, an empirical relationship that fits the observed pH dependence of T_t was introduced [64].

$$T_t = f_{depro}T_{depro} + (1 - f_{depro})T_{pro} \qquad (8)$$

where f_{depro} is the fraction of total ELP guest residues that is deprotonated.

T_t at intermediate pH can be linear interpolated between T_t of a fully deprotonated ELP at a high pH, T_{depro}, and a fully protonated ELP at a low pH, T_{pro}. This relationship is strongly supported by previous observations [5]. A Henderson-Hasselbalch relationship can be used to determine f_{depro} [64]:

$$pH = pKa + \log |\frac{C_{depro}}{C_{pro}}| \quad (9)$$

$$C_{depro} + C_{pro} = C_{total} \quad (10)$$

where C_{depro} and C_{pro} are concentration of deprotonated and protonated ionizable residues, respectively.

Substitute Equation 9 and 10 into Equation 8, we can write:

$$T_t = T_{pro} + \frac{T_{depro} - T_{pro}}{10^{(pKa-pH)} + 1} \quad (11)$$

This model (Equation 11) directly describes the effect of pH on T_t. T_{pro}, T_t of nonionic ELP, could be calculated by using the original model, Equation 1, and the parameters from Table 3.1. The only unknown in this model is T_{depro}.

It was shown previously that Equation 11 and 1 can be combined [64]:

$$T_t = T_{cr,pro} + \frac{K_{pro}}{L} \ln\left[\frac{C_{cr}}{C}\right] + \frac{T_{cr,depro} - T_{cr,pro} + \frac{(K_{depro} - K_{pro})}{L}(\ln\left[\frac{C_{cr}}{C}\right])}{1 + 10^{(\mathrm{pKa-pH})}} \quad (12)$$

where $T_{cr,pro}$ and $T_{cr,depro}$ are molar critical temperature for the protonated and deprotonated ELPs, respectively. K_{depro} and K_{pro} are length-concentration interaction parameters, and they are dependent on pH as well [11]. An important assumption of final equation is that the critical temperatures of protonated and deprotonated ELPs are the same [64].

Experimental data of T_t versus [C] at high pH (Figure 3.7) were fit by Equation 12 to determine unknown parameters (Table 3.2).

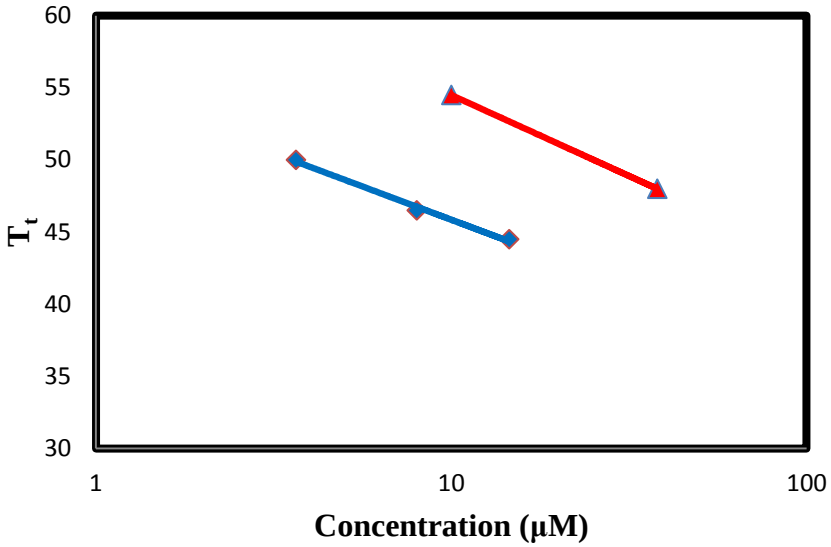

Figure 3.7: T_t versus log[C] of $(VEV)_{12}$-foldon at pH4.2; T_t versus log[C] of $(VEV)_{12}$ at pH 3.8.

Table 3.2: Multiple parameters describing the dependence of the transition temperature on concentration and pH:

ELPs	pK_a	$T_{cr,\,pro}$ (˚C)	$T_{cr,\,depro}$ (˚C)	K_{pro} (˚C)	K_{depro} (˚C)
$(VEV)_{12}$	4.8	19.2	80.4	163	297
$(VEV)_{12}$-foldon	4.8	18.2	61.1	365	701

Up to this point, all parameters were determined by using T_t versus ELP concentrations at different pH, which allow us to calculate T_{depro} of a given ELP at specific concentration.

3.5 T_t versus pH

Transition temperature of linear and trimer ELPs were measure at a fixed concentration over a range of pH (Figure 3.8).

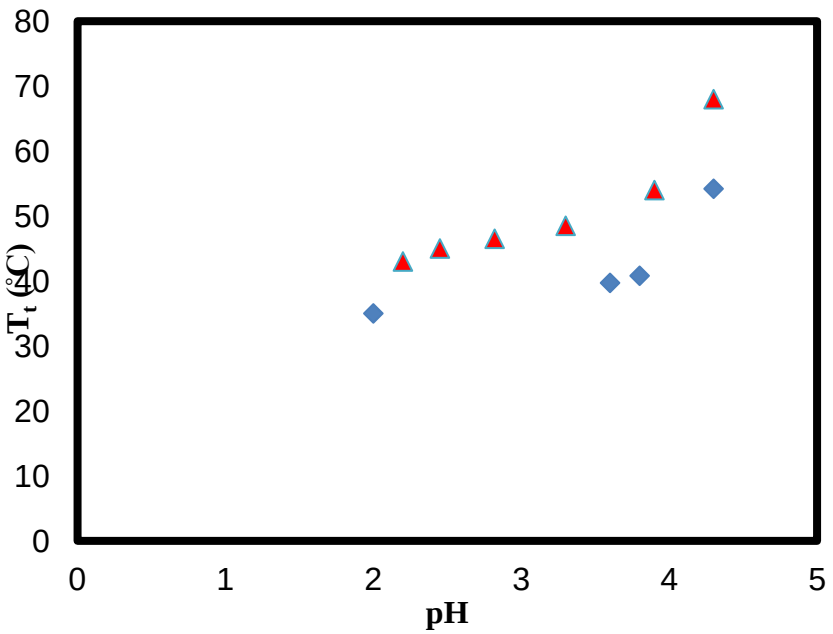

Figure 3.8: T_t as a function of pH, concentration of linear ELPs is 10 μM (triangles), concentration of trimer ELPs is 3.3 μM (diamond).

Before comparing best fits and our experimental data, it is interesting to notice that trimer ELP has a lower T_t than linear one at the same pH even at lower molar concentration. Previous studies have shown that, incorporation of foldon domain, which derived from the native T4 phage fibritin, can significantly improve thermostability of collagens and peptides at different solution condition [57]. Those conditions included low concentration and the addition of certain amount of guanidine chloride [56]. The result of this measurement indicated that foldon could also improve the thermostability of charged

ELPs. Besides compositions, chain length and concentration, the fusion of a foldon domain to the C-terminus of ELPs gives another method to tune the transition temperature of charged ELPs.

Experimental data of T_t versus [C] was fit into Equation 11 to determine estimated T_{pro} and T_{depro} (Table 3.3) at specific concentration, using a pK_a of linear and trimer ELP equal to 4.8, which was determined from titration (data not shown here).

Table 3.3: Estimated T_t of fully protonated and deprotonated ELPs at fixed concentration

ELPs	T_{pro} (˚C)	T_{depro} (˚C)
$(VEV)_{12}$, 10 μM	46.7	131.1
$(VEV)_{12}$-foldon, 3.3 μM	38.1	98.8

These parameters were used to fit data as a function of pH (Figure 3.9).

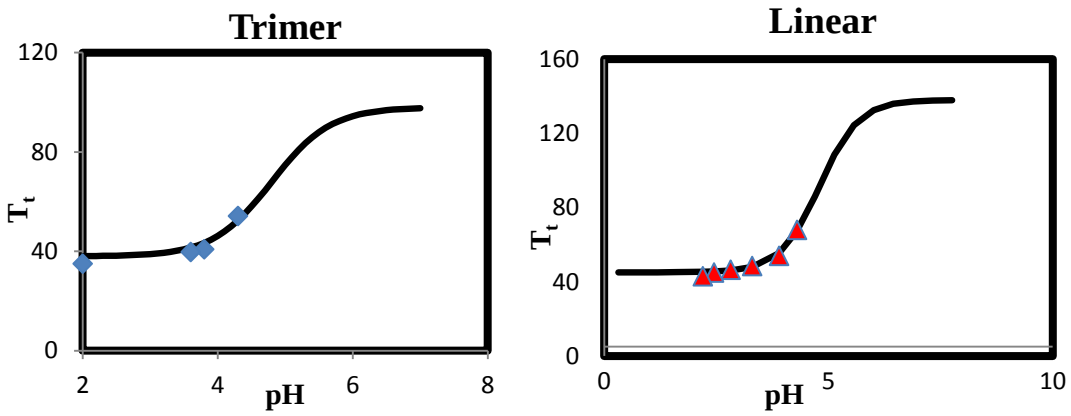

Figure 3.9: pH dependence of ELP phase transition temperature. Best-fit curves following equation 11 have been shown (lines).

T_{pro} and T_{depro} of linear and trimer ELPs which were fit from concentration dependence data, have been used to describe T_t as a function of pH. Impressively, this model describes most of our experimental data for both linear and trimer ELPs. Experimental data of T_t versus pH was fit to Equation 11 (Table 3.4) to validate estimated values,

Table 3.4: T_t of pH data fit to equation 11 and parameters as reported

ELPs	T_{pro} (˚C)	T_{depro} (˚C)
$(VEV)_{12}$, 10 μM	44.4	141
$(VEV)_{12}$-foldon, 3.3 μM	34.5	115

Based on this analysis, T_{pro} determined from T_t versus pH is about 2 to 4 ˚C lower than to parameters determined from T_t versus [C] for linear and trimer ELPs. T_{depro} determined from T_t versus pH is 10 to 20 ˚C higher than T_{depro} determined from T_t versus [C]. This difference may be caused by the fact that volume concentration was used to calculate the value of the molar critical point. To use volume concentration to determine parameters of ELPs with different chain length could give better fit parameters.

Even with this difference, this model still describes the relationship between T_t and pH quite well. It also permits the selection of the best length and mixture of guest residues to trigger phase transition of ELP at a designed pH.

3.6: T_t versus Salt Concentration

Previous studies on non-charged ELPs, $(GVGVP)_n$, have shown that the addition of NaCl causes a decrease in transition temperature and an increase in ΔH [63]. The inverse temperature transition is a complex and multistep transition [58]. In aqueous solution, some of the processes are endothermic, likely associated with the loss of hydrophobic hydration, while others, like self-assembly, are exothermic [58]. The technique used to separate these two overlapping processes is temperature modulated differential scanning calorimetry (TMDSC). And result indicates that magnitude of the exothermic component is less than one third of the endothermic component [65].

Both the endothermic and exothermic components increase as [NaCl] increases [65]. The effect of the increase in [NaCl] in the thermal parameter is equivalent to an increase in the hydrophobicity of the polymer chain. As it has been shown before, increase in hydrophobicity causes the decrease in T_t and increase in ΔH (5) [11]. Experimental data of the effect [NaCl] on T_t of acidic ELPs at protonated state is presented in Figure 3.10.

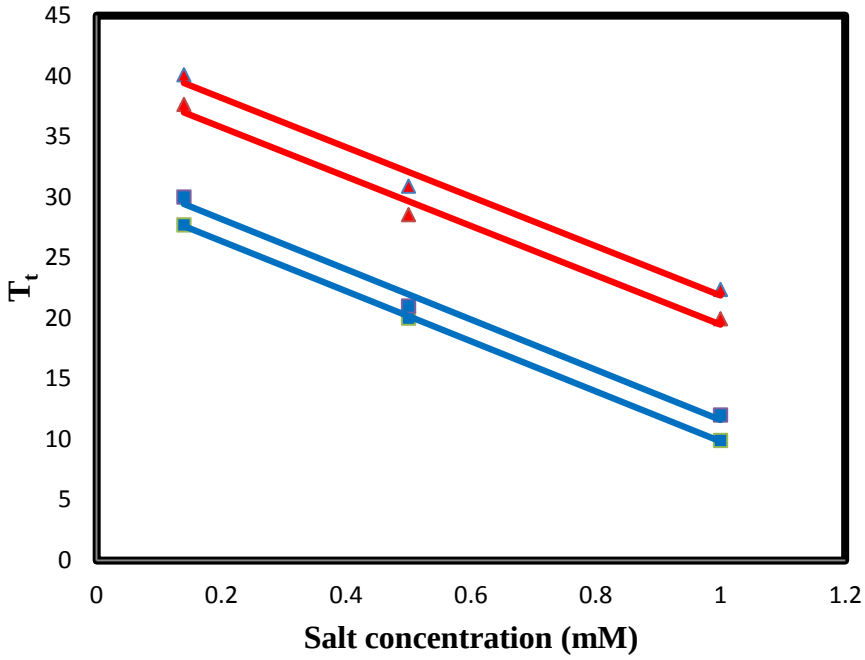

Figure 3.10: $(VEV)_{12}$ (triangle) and $(VEV)_{12}$-foldon (square): T_t versus [NaCl] at pH 2.7.

Both ELP configurations were measure at pH 2.7, where the ionic groups were fully protonated. Therefore, the salt effect on T_t of $(GVGVP)_n$ would be similar as that on protonated acidic ELPs. There is a linear decrease in T_t versus [NaCl]; a similar fashion has been reported by other studies [9, 63]. Also, T_t undergoes a sharp decline with the addition of NaCl. Linear and trimer ELPs were measured at different concentration, resulting in four curves with approximately the same slope. An equation could be developed to indicate the relationship between [NaCl] and T_t (Equation 12).

$$T_t = T_0 + C[M] \qquad (12)$$

This equation was originally developed by Cho and his colleges [2]. Where T_0 is T_t at 0 M of [NaCl]. C is the constant with a unit of ˚C/M; [M] is the concentration of salt

in the solution. In the equation, constant C is the slope of the curve. These four measurements suggest that C is independent of protein constructs and concentration. For acidic ELPs at protonated state, the addition of NaCl has a similar effect as that of non-charged ELPs.

A similar measurement was performed at pH 3.9 for $(VEV)_{12}$. The slope of the curve is slightly different from that at pH 2.7 (Figure 3.11).

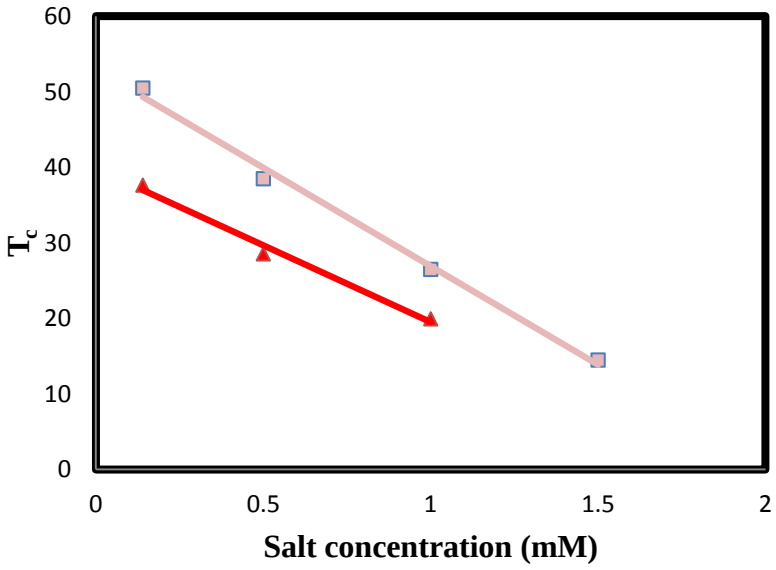

Figure 3.11: Comparison between $(VEV)_{12}$ at pH 2.7 (triangle) and $(VEV)_{12}$ at pH 3.9 (square).

At higher pH, the curve remains the linear fashion with a steeper slope. With the same amount of changes in [NaCl], the T_t of more charged ELP drops faster. A potential explanation could be that at higher pH, electrostatic interaction between Na^+ and COO^- is engaging in the system, the ionic binding between COO^- and Na^+ is stronger than

charge-dipole interaction between COO^- and water molecules. With this shielding effect, a decrease in hydrophility causes a decrease in T_t. At the same time, the effect of NaCl on hydrophobic residues is still remaining. Therefore, the addition of NaCl has two effects on charged ELPs, leading to a sharper change in T_t.

CHAPTER IV

CONCLUSIONS

In this work, we have synthesized two acidic ELPs with different configurations, which both have the pH-responsive ability. One acidic ELP is linear $(VEV)_{12}$, the other one is a three-armed star polymer, $(VEV)_{12}$-foldon. The addition of foldon domain to linear ELPs leads to a trimer structure in solution and causes a change in the value of T_t. The results showed, in either charged or non-charged state, ELP with foldon has a lower transition temperature in similar solution conditions. A previous empirical model for linear charged ELPs was used to describe the transition temperature of $(VEV)_{12}$ as a function of concentration and pH. Volume concentration was introduced to this model to determine the empirical critical point. Impressively, this model describes pH-responsive ELPs with two different configurations quite well.

It has been reported that ELP with foldon domain can form micelles at certain conditions [47]. This model provides a quantitative method for rational design of pH-responsive trimer ELPs whose transition can be trigger at a specified pH.

REFERENCES

[1] Rodriguez-Cabello, J.C., J. Reguera, A. Girotti, F.J. Arias, M. Alonso, Genetic engineering of protein-based polymers: the example of elastinlike polymers. *Adv. Polym. Sci*, **2006,** 200, 119–167.

[2] Cho Y, Zhang Y, Christensen T, Sagle LB, Chilkoti A, Cremer PS. Effects of Hofmeister anions on the phase transition temperature of elastin-like polypeptides. *J. Phys. Chem. B*, **2008**, 113, 13765-13771

[3] Ghandehari, H.; Cappello, Genetic engineering of protein-based polymers: potential in controlled drug delivery. *J. Pharmaceutical Research*, **1998**, 15, 813-815.

[4] Urry, D.W., Free energy transduction in polypeptides and proteins based on inverse temperature transitions. *Progress in Biophysics & Molecular Biology*, **1992**, 57, 23-57.

[5] Urry, D.W. Physical Chemistry of Biological Free Energy Transduction As Demonstrated by Elastin Protein-Based Polymers. *J. Phys. Chem. B*, **1997**, *101*, 11007-11028.

[6] Freire, E. The thermodynamic linkage protein structure, stability, and function. *Methods Mol. Biol*, **2001,** 168, 37-68.

[7] Urry. D. W. *Prog. Biophys. molec. Biol*, **1992**, 57, 23-57.

[8] Betre, H.; Ong, S. R.; Guilak, F.; Chilkoti, A.; Fermor, B.; Sectton, L. A. Chondrocytic differentiation of human adipose-derived adult stem cells in elastin-like polypeptide. *Biomaterials*, **2006**, 27, 91-9.

[9] Yamaoka T, Tamura T, Seto Y, Tada T, Kunugi S, Tirrell DA. Mechanism for the phase transition of a genetically engineered elastin model peptide $(VPGIG)_{40}$ in aqueous solution. *Biomacromolecules*, **2003**, 4, 1680-1685.

[10] Urry DW, Haynes B, Zhang H, Harris RD, Prasad KU. Mechanochemical coupling in synthetic polypeptides by modulation of an inverse temperature transition. *Proc. Nadtl. Acad. Sci. USA*, **1988**, 85, 3407-3411.

[11] Dominic Chow, Michelle L. Nunalee, Dong Woo Lim, Andrew J. Simnick, Ashutosh Chilkoti. Peptide-based biopolymers in biomedicine and biotechnology. *Materials Science & Engineering R-reports*, **2008** vol. 62, no. 4, pp. 125-155.

[12] Simnick AJ, Lim DW, Chow DC, Chilkoti A. Biomedical and Biotechnological Applications of Elastin-Like Polypeptides. *Journal of Macromolecular Science, Part C: Polymer Reviews*, **2007**,47, 121–154.

[13] Nath, N. and Chilkoti, A. Creating 'smart' surfaces using stimuli responsive polymers. *Advanced Materials*, **2002,** 14,1243.

[14] M.E. Harmaon, M Tang & CW Frank, Fast-responsive semi-interpentrating hydrogel networks imaged with confocal fluorescence microscopy. *Polymer*, **2003**, 44, 4547-4556.

[15] A.T. Florence, D. Attwood, *Physicochemical Principle of Pharmacy*, *3rd ed*., Macmillam Press, London, **1998**, 380.

[16] Kim J-H, Lee TR. Thermo- and pH-Responsive Hydrogel-Coated Gold Nanoparticles. *Chemistry of Materials*, **2004**, 16, 3647.

[17] Nakayama, M.; Okano, T.; Miyazaki, T.; Kohori, F.; Sakai, K.; Yokoyama, M. *Journal of Controlled Release*, **2006**, 115, 46.

[18] Siegel, R.A., "Hydrophobic Weak Polyelectrolyte Gels: Studies of Swelling Equilibria and Kinetics," *Adv. Polym. Sci **1993,*** 109, 233-267.

[19] S.J. Hollister, Scaffold Design and Manufacturing: From Concept to Clinic, *Adv. Mater*. 21 **2009,** 3330–3342.

[20] R. Langer, L.G. Cima, J.A. Tamada, E. Wintermantel, Future-directions in biomaterials, *Biomaterials* 11 **1990**, 738–745.

[21] R. Langer, J.P. Vacanti, Tissue engineering, *Science* 260 **1993**, 920–926

[22] Panitch, A.; Yamaoka, T.; Fournier, M.J.; Mason, T.L; Tirrell, D. A., Design and biosynthesis of elastin-like artificial extracellular matrix proteins containing periodically spaced fibronectin CS5 domains. *Macromolecules* **1999**, 32, 1701-1703.

[23] Trabbic-Carlson K, Setton LA, Chilkoti A. Swelling and mechanical behaviors of chemically cross-linked hydrogels of elastin-like polypeptides. *Biomacromolecules* **2003**, 4, 572-580.

[24] Urry, D. W. Entropic elastic processes in protein mechanisms. I. Elastic structure due to an inverse temperature transition and elasticity due to internal chain dynamics. *J. Phys. Chem*. **1988**, 7, 1-34.

[25] McMillan, R. A.; Conticello, R. P. Macromolecules **2000**, 33, 4809-4821.

[26] Girotti A, Reguera J, Rodríguez-Cabello JC, Arias FJ, Alonso M, Matestera A. Design and bioproduction of a recombinant multi(bio)functional elastin-like protein polymer containing cell adhesion sequences for tissue engineering purposes. *Journal of Materials Science-Materials in Medicine*, **2004**, 15: 479-484.

[27] Urry DW, Trapane TL, Prasad KU. Phase-structure transitions of the elastin polypentapeptide-water system within the framework of composition-temperature studies. *Biopolymer*, **1985**, 24:2345-2356.

[28] Meier S, Güthe S, Kiefhaber T, Grzesiek S. Foldon, the natural trimerization domain of T4 fibritin, dissociates into a monomeric A-state form containing a stable beta-hairpin: atomic details of trimer dissociation and local beta-hairpin stability from residual dipolar couplings. *J. Mol. Bio*, **2004,** 344, 1051-1069.

[29] D.E. Meyer, A. Chilkoti, Genetically Encoded Synthesis of Protein-Based Polymers with Precisely Specified Molecular Weight and Sequence by Recursive Directional Ligation: Example from Elastin-like Polypeptide System, Biomacromolecules, 2002, 3, 367.

[30] L. H. Sperling, Introduction to Physical Polymer Science. Fourth edition ed. Wiley: **2006.**

[31] Ali Ghoorchian , James T. Cole and Nolan B. Holland, *Macromolecules*, **2010**, 43 (9), 4340–4345.

[32] A. A. Chmiel, J. M. Bujnicki, & K. J. Skowronek, A homology model of restriction endonuclease SfiI in complex with DNA, *BMC Structural Biology*, **2005, 2,** 2: 2-11.

[33] Taylor, L. D.; Cerankoesky, L. D. *J. Polym. Sci., Part B*, **1975**, 13, 2551.

[34] McPherson, D. T.; Xu, J.; Urry, D. W. Product purification by reversible phase transition following Escherichia coli expression of genes encoding up to 251 repeats of the elastomeric pentapeptide GVGVP. *Protein Expr. Purif*, **1996**, 7, 51-57.

[35] P. Vohl, Photogr. Surface photovoltage effects in titanium dioxide films. *Sci. Eng*, **1960,** 13, 120.

[36] Meyer, D. E.; Chilkoti, A. Purification of recombinant proteins by fusion with thermally-responsive polypeptides. *Nat. Biotechnol*, **1999**, 17, 1112-1115.

[37] Urry, D.W., Free energy transduction in polypeptides and proteins based on inverse temperature transitions. *Progress in Biophysics & Molecular Biolo*gy **1992**, 57 (1), 23-57.

[38] *Macromolecules*, **2010**,43, 9.

[39] LA Strzegowski, MB Martinez, DC Gowda, DW Urry & DA Tirrell, *Journal of American Chemical Society* **1994**, 116, 813-814.

[40] Eds. N Ashammakhi, R Reis & E Chiellini. *Topics in Tissue Engineering*, **2007,** 3.

[41] Gill SC, von Hippel PH. Calculation of protein extinction coefficients from amino acid sequence data. *Analytical Biochemistry*, **1989,** 182, 319-326.

[42] Naclerio G, Falasca A, Petrella E, Nerone V, Cocco F, Celico F. Potential role of Bacillus endospores in soil amended by olive mill wastewater. *Biomolecules*, **2010**, 11, 2873-2879.

[43] Urry DW, Parker TM, Reid MC, Gowda DC. *J Bioactive Comp Polym*, **1991**, 6:23.

[44] Urry DW, What sustains life? Consilient mechanisms for protein-based machines and materials. *Springer, Berlin Heidelberg New York,* **2005.**

[45] Johnson, M. J. Isolation and properties of a pure yeast polypeptide. *J. Biol. Chem*., **1941**, 137, 575–586.

[46] Yeh, C.S. *Microchem. J*. **1996,** 11, 229-236.

[47] Ghoorchian A, Holland NB. Molecular architecture influences the thermally induced aggregation behavior of elastin-like polypeptides. *Biomacromolecules*, **2011**, 12 (11), 4022-4029.

[48] McPherson DT, Morrow C, Minehan DS, Wu J, Hunter E, Urry DW. Production and purification of a recombinant elastomeric polypeptide, G-(VPGVG)19-VPGV, from Escherichia coli. *Bitechnol. Prog*, **1992**, 8, 347-352.

[49] Jan Kostal, Ashok Mulchandani, and Wilfred Chen. Tunable Biopolymers for Heavy Metal Removal. *Macromolecules*, **2001**, 34, 2257-2261.

[50] Elizabeth R. Wright, R. Andrew McMillan, Alan Cooper, Robert P. Apkarian, and Vincent P. Conticello. Self-Assembly of Hydrogels From Elastin-Mimetic Block Copolymers. *Macromolecules*, **1999**, 32, 3643-3648.

[51] Ghoorchian Ali, Doctoral dissertation, Cleveland State University (**2012**)

[52] Güthe S, Kapinos L, Möglich A, Meier S, Grzesiek S, Kiefhaber T. Very fast folding and association of a trimerization domain from bacteriophage T4 fibritin. *J. Mol. Biol*, **2004**, 337, 905-915.

[53] Yizhi Tao, Sergei V Strelkov, Structure of bacteriophage T4 fibritin: a segmented coiled coil and the role of the C-terminal domain. *Structure,* **1997**, 5:789-798

[54] Frank S, Kammerer RA, Mechling D, Schulthess T, Landwehr R, Bann J, Guo Y, Lustig A, Bächinger HP, Engel J.Stabilization of short collagen-like triple helices by protein engineering. *J. Mol.Biol*, **2001**, 208, 1081-1089.

[55] Dan E. Meyer and Ashutosh Chilkoti, Quantification of the effects of chain length and concentration on the thermal behavior of elastin-like polypeptides. *Biomacromolecules*, **2004**, 5, 846–851.

[56] Naclerio G, Falasca A, Petrella E, Nerone V, Cocco F, Celico F. Potential role of Bacillus endospores in soil amended by olive mill wastewater. *Biomacromolecules* **2010**, 11, 2873-2879.

[57] Bhardwaj A, Walker-Kopp N, Wilkens S, Cingolani G. Foldon-guided self-assembly of ultra-stable protein fibers. *Protein Science* **(2008)**, 17,1475-1485.

[58] Reguera, J,; Lagaron, J.M.; Alonso, M.; Reboto, V.; Calvo, B.; Rodriguez-Cabello, J. C. *Macromolecules* **2003**, 36,8470-8476.

[63] J. Reguera, D.W. Urry, T.M. Parker, D.T. McPherson, J.C. Rodriguez Cabello, Effect of NaCl on the Exothermic and Endothermic Components of the Inverse Temperature Transition of a Model Elastin-like Polymer, *Biomacromolecules*, **2007, 8,** 358.

[64] J. Andrew MacKay, Daniel J. Callahan, Kelly N. FitzGerald, and Ashutosh Chilkoti. Quantitative Model of the Phase Behavior of Recombinant pH-Responsive Elastin-Like Polypeptides, *Biomacromolecules*, **2010,** 11, 2873-2879.